Absorption and fluorescence study of an antiferromagnet with alternating strong and weak coupling : RbMnCl3

R. Moncorgé, B. Briat, J.C. Canit

Classification
Physics Abstracts
66.30 — 78.55

Absorption and fluorescence study of an antiferromagnet with alternating strong and weak coupling : $RbMnCl_3$

R. Moncorgé

Physicochimie des Matériaux Luminescents (*), Université de Lyon I,
43 bd du 11 Novembre 1918, 69622 Villeurbanne, France

B. Briat and J. C. Canit

Laboratoire d'Optique Physique de l'ESPCI (**), 10, rue Vauquelin, 75231 Paris Cedex 05, France

(*Reçu le 12 janvier 1984, accepté le 21 mars 1984*)

Résumé. — Le spectre d'absorption de $RbMnCl_3$ présente des raies magnon chaudes (75, 70 et 31 cm^{-1}) et froides (70, 65, 54 et 45 cm^{-1}). Les énergies réduites ($E/|J_2|$) des magnons de bord de zone sont calculées en fonction du rapport J_1/J_2 des deux intégrales d'échange caractérisant ce matériau. L'analyse de nos résultats conduit à $J_1/J_2 \simeq 6$ et $J_1 \simeq 26$ cm^{-1}, en sérieux désaccord avec des résultats antérieurs. Nos mesures de fluorescence prouvent que l'excitation optique reste localisée.

Abstract. — The absorption spectrum of $RbMnCl_3$ shows hot magnon satellites with frequencies of 75, 70 and 31 cm^{-1}, and cold bands with frequences of 70, 65, 54 and 43 cm^{-1}. The reduced zone boundary magnon energies ($E/|J_2|$) are expressed in terms of the ratio of the strong (J_1) and weak (J_2) exchange coupling constants. The fit of our experimental data leads to $J_1/J_2 \simeq 6$ and $J_1 \simeq 26$ cm^{-1}, in serious disagreement with previous findings. Fluorescence measurements prove that optical excitations are completely localized.

1. Introduction.

In the recent years, many efforts have been devoted to the investigation of the magnetic properties of the hexagonal compound $RbMnCl_3$. This is because this material might belong to a class of antiferromagnets in which alternating strong and weak exchange interactions J_1 and J_2 connect the neighbouring magnetic moments. For very distinct exchange coupling constants, it is known [1] that the simple molecular field approximation and the conventional spin-wave analysis do not apply satisfactorily since they lead to unphysical results. In this situation, a better treatment consists in solving the eigenstates of the exchange Hamiltonian for the strongly coupled pairs of magnetic ions and then taking into account the remaining weak exchange interactions through the effective field approximation. Using this approach, Japanese workers [2, 3] have fitted their magnetization data with $J_1/J_2 = 10$ and $J_1 = -29.4$ cm^{-1} [4]. However when use is made of their theoretical plot giving $T_N/|J_1|$ as a function of J_2/J_1, the above mentioned experimental values do not lead to the right ordering temperature $T_N \simeq 94$ K.

The study of the optical absorption spectrum of $RbMnCl_3$ in its ordered phase should help to answer this question since bands connected with the exciton-magnon absorption mechanism can give direct information about the magnon spectrum itself. A number of observations are already available in the past literature. In this communication, we add some of our own concerning the hot magnon sidebands which allow us to determine more precisely the frequencies of the magnons at the Brillouin zone (B.Z.) boundaries. We then make the connection with the existing theories mentioned above to set realistic values for the various exchange integrals and to give a plausible description of the whole magnon spectrum. Finally, we examine the effect of the magnetic structure of $RbMnCl_3$ on its fluorescence dynamics.

(*) ERA 1003 C.N.R.S.
(**) ER. 5 C.N.R.S.

2. Crystallomagnetic properties of $RbMnCl_3$.

Large single crystals were prepared by the Bridgman technique, using a stoichiometric mixture of anhydrous halides. The starting materials $MnCl_2.4\,H_2O$ (Merck, Ref. 5927) and RbCl (Merck, Ref. 7622) had a low content of impurities (less than 10 ppm for each of them) and were not purified further.

At room temperature, the crystal structure of $RbMnCl_3$ is hexagonal, space group D^4_{6h}, with six formula units per unit cell and $a = b = 7.16$ Å, $c = 17.79$ Å. The unit cell contains two types of manganese sites, one third being centrosymmetric and labelled Mn 1 (site group D_{3d}), and two thirds being non centrosymmetric and labelled Mn 2 (site group C_{3v}). In this paper, we shall be concerned with Mn 2 sites only.

At 270 K, the crystal undergoes [5] a second-order ferroelastic structural phase transition and the optical axis is lost. Although this posed no inconveniences for our study of the absorbance *versus* temperature, this prevented us from using more sensitive techniques such as magnetic circular or linear dichroism.

Below $T_N \simeq 94$ K, the crystal orders antiferromagnetically and the spins align in ferromagnetic planes which alternate along the hexagonal axis (see Fig. 1 of Ref. 1a). The adjacent Mn 2 ions interact *via* the exchange coupling J_1, and each Mn 2 pair-ion interacts with three neighbouring Mn 1 ions *via* the exchange coupling J_2. The effective fields responsible for magnetic exchange and anisotropy are given by $H_E \simeq (860 \pm 40)$ kOe and $H_A = (60 \pm 10)$ kOe [6].

3. Optical properties of $RbMnCl_3$.

The crystal used for absorption experiments was 0.26 mm thick and cut perpendicular to the trigonal axis. Light therefore always propagated along the (high temperature phase) unique axis. Figure 1 shows a low temperature survey spectrum, together with the nomenclature used hereafter. Except for A and B, each band is characterized (see Figs. 2-5) by a broad multiphonon feature and a series of sharp lines which occur on its low energy side at low temperature. Among these lines one can distinguish between pure and phonon — or magnon — assisted exciton transitions and among the latter between « hot » and « cold » magnon sidebands. The cold absorption process corresponds to the simultaneous creation of an exciton and a magnon in antiparallel magnetic sublattices. Since they coexist in time the exciton and the magnon may interact and the shape of the

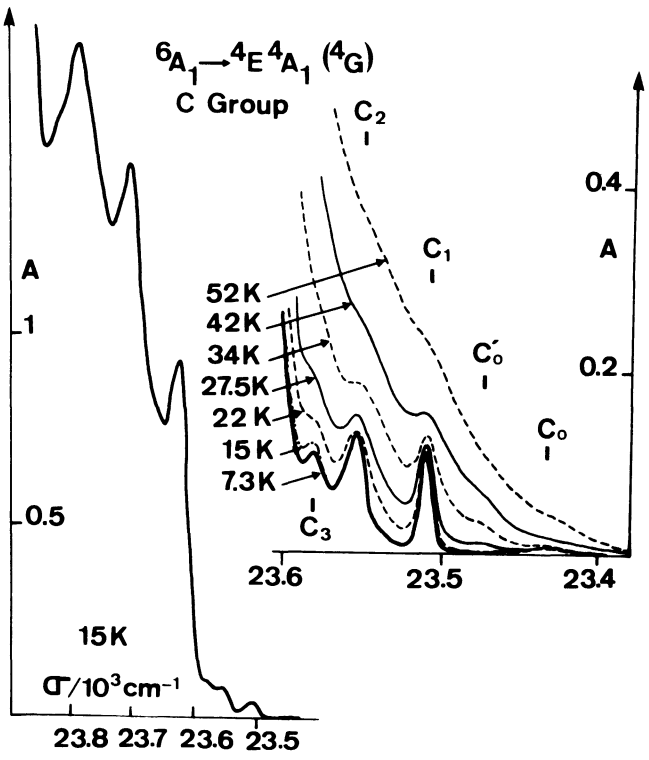

Fig. 2. — Detail of the axial spectrum *versus* temperature for the C group of bands. The spectral band-width chosen was $\Delta\lambda = 0.75$ Å.

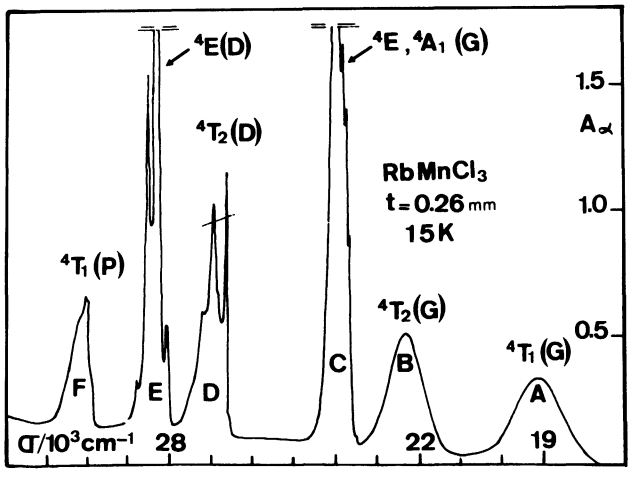

Fig. 1. — Survey of the « axial » absorption spectrum of $RbMnCl_3$ under 0.26 mm and at 15 K. The nomenclature refers to the octahedral group notations.

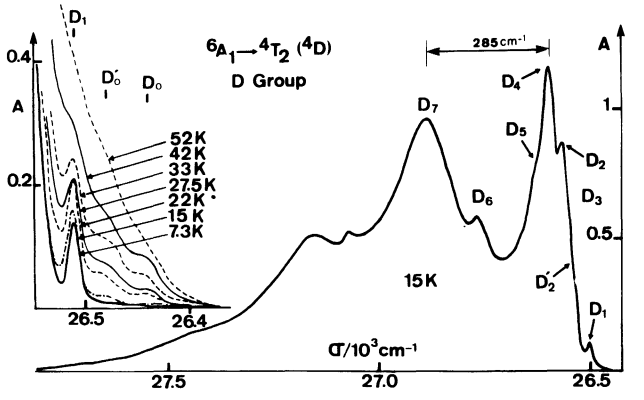

Fig. 3. — Axial spectrum *versus* temperature for the D group. $\Delta\lambda = 0.75$ Å. The D_4-D_7 splitting corresponds to the totally symmetric Raman mode of highest energy [10].

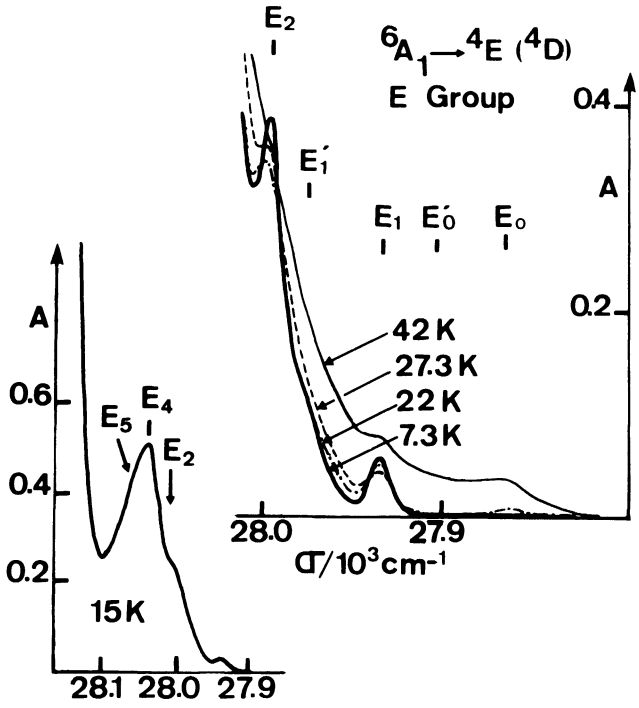

Fig. 4. — Axial spectrum *versus* temperature for the E group. $\Delta\lambda = 0.75$ Å.

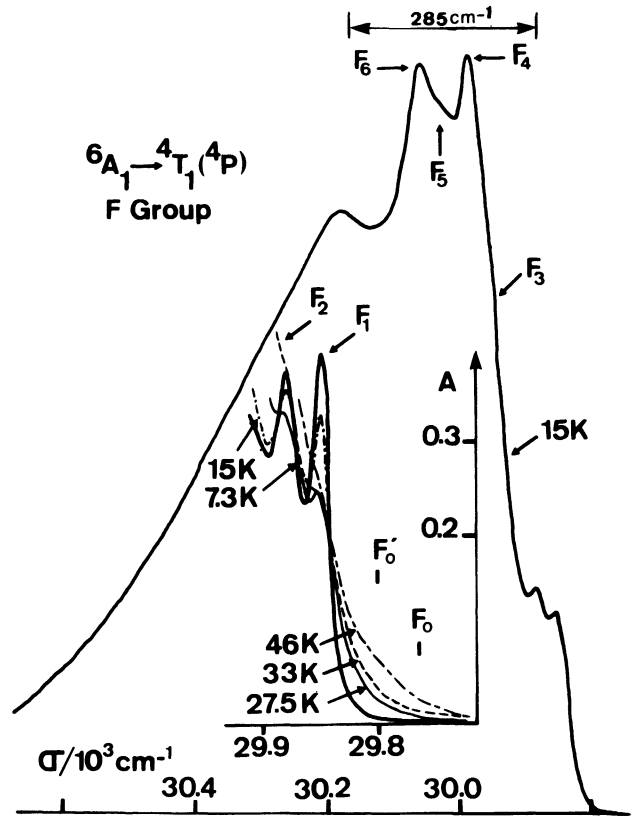

Fig. 5. — Axial spectrum *versus* temperature for the E group. $\Delta\lambda = 0.75$ Å. Bands F_0 and F'_0 occur only as overlapping shoulders.

magnon sideband which should reflect the exciton and magnon densities of states, may be significantly distorted [7]. The observed magnon interval is generally smaller (few cm^{-1}) than the true B.Z. magnon energy. In a hot absorption process an exciton is created and a magnon is annihilated on the same sublattice. In this case the magnon sideband is almost free of any exciton-magnon interaction. This allows us to determine precisely the frequencies of the magnons on the B.Z. boundary where the density of states is highest.

A detailed analysis of the fine structure was first reported by Popkov *et al.* [8] for group C. They found magnon frequency intervals (α spectrum) of 46 and 71 cm^{-1} from the cold magnon sidebands, and of 75 cm^{-1} from the hot ones. Belyaeva *et al.* [9, 10] extended the analysis to the other groups. They observed no hot magnon satellite besides those already mentioned at 75 cm^{-1} in the C group but they reported frequency intervals of 46, 56, 62-65 and 70 cm^{-1} (cold magnon satellites).

Our own data are shown in great detail in figures 2-5 and are collected in table I together with those of Belyaeva's group. The two sets of data have been standardized by considering the energy of the better resolved line for each group of bands. All the features reported previously were indeed clearly observed in our experiments. Furthermore, we provide new information concerning five hot bands (C'_0, E_0, E'_0, F_0 and F'_0) and one cold band (E'_1). The spacings shown in table I are correct to within $\pm$ 2 cm^{-1}, except perhaps for the few bands appearing as shoulders (Sh), for which the accuracy is somewhat lower. This uncertainty is due to the broadness of exciton-magnon bands (see Figs. 2-5).

In summary, hot magnon satellites occur with characteristic frequencies of 75 cm^{-1} (C_0), 70 cm^{-1} (D, E_0) and 31 cm^{-1} (C'_0, E'_0) while cold bands are seen with frequencies of 70 cm^{-1} (C_3), 65 cm^{-1} (E_2, F_3), 54 cm^{-1} (D_2, D_4) and 45 cm^{-1} (C_2, E'_1).

Our fluorescence data are shown in figure 6. These data have been obtained by exciting the sample with lasers of moderate intensities, either with a C.W. argon pump dye laser of $\sim$ 100 mW unfocused at 5 500 Å or with a 10 Hz pulsed frequency doubled YAG : Nd laser with $\sim$ 100 μJ per pulse unfocused at 5 320 Å. The emission band is broad, extends from 5 700 to 7 000 Å and peaks around 6 250 Å. In spite of a careful search, we were unable to observe any sharp features on its blue side, even at the lowest temperature $T = 1.5$ K. This contrasts with Kambli's data [11] and certainly indicates that the sample grown in Bern is of better quality than ours.

Following a pulsed dye laser excitation, the fluorescence decays exponentially (Fig. 6b) with the time constant $\tau \simeq 1.1$ ms at $T = 1.5$ K for any emission wavelength selected across the emission band. The integrated emission intensity and the fluorescence lifetime decrease very smoothly when the temperature is

Table I. — *Energy of the absorption bands of hexagonal* $RbMnCl_3$ *and their interpretation in terms of acoustic* (a) *or optical* (o) *magnon modes. sh stands for « shoulder ».*

	Data from ref. [9, 10]	Our results	Nomenclature	Energy intervals	Magnon assignment
C group	23434	23435	C_0	$\nu_1 - 75$	$E_{oA\uparrow}$
	—	23478	C'_0	$\nu_1 - 32$	E_{aA}
	23510	23510	C_1	ν_1	
	23556	23553	C_2	$\nu_1 + 43$	$E_{oA\downarrow}$
	23575 / 23582	23580	C_3	$\nu_1 + 70$	$E_{oK,oM}$ or $E_{oA\uparrow}$
D group	26440	26442	D_0	$\nu_1 - 70$	$E_{oK,oM}$
	26478	26480	D'_0	$\nu_2 - 70$ or $\nu_1 - 32$	$E_{oK,oM}$ or E_{aA}
	26512	26512	D_1	ν_1	
	26550	26550	D'_2 (sh)	ν_2	
	26568	26566	D_2	$\nu_1 + 54$	E_{aM} or E_{aK}
	26582	26582	D_3 (sh)	$\nu_1 + 70$ or $\nu_2 + 32$	$E_{oK,oM}$ or E_{aA}
	26606	26603	D_4	$\nu_2 + 53$	E_{aM}
	26644	26645	D_5 (sh)		
E group	—	27863	E_0	$\nu_1 - 70$	$E_{oK,oM}$
	—	27903	E'_0 (sh)	$\nu_1 - 30$	E_{aA}
	27933	27933	E_1	ν_1	
	—	27980	E'_1 (sh)	$\nu_1 + 47$	$E_{oA\downarrow}$
	27997	27999	E_2	$\nu_1 + 65$	$E_{oK,oM}$
	28034	28037	E_4		
	28058	28062	E_5		
F group	—	29770	F_0 (sh)	$\nu_1 - 77$	$E_{oA\uparrow}$
	—	29800	F'_0 (sh)	$\nu_1 - 77$	$E_{oA\uparrow}$
	29847	29847	F_1	ν_1	
	29879	29877	F_2	ν_2	
	29949	29942	F_3	$\nu_2 + 65$	$E_{oK,oM}$
	29969	29969	F_4		
	30007	30004	F_5		
	30042	30034	F_6		

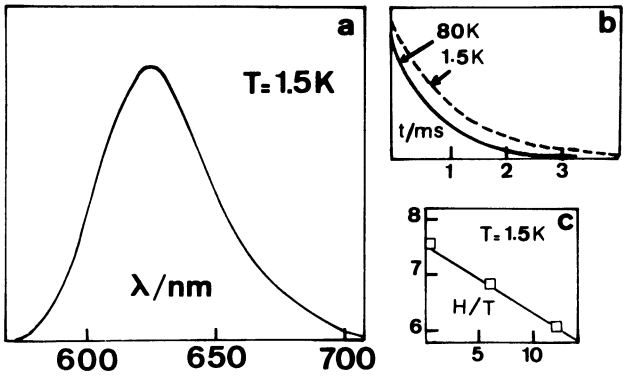

Fig. 6. — Fluorescence data for $RbMnCl_3$: a) Emission spectrum at 1.5 K. The argon laser was directed perpendicular to the (high temperature) c axis and unpolarized light was collected also at a right angle to c. b) Fluorescence decay mode at 80 K (τ = 0.82 ms) and 1.5 K (τ = 1.12 ms). c) Emission intensity *versus* the strength of a magnetic field $B \perp c$.

increased up to about 80 K. Also the emission intensity decreases quite significantly when a strong magnetic field is applied perpendicularly to the c axis in the plane of the spins. In this experiment the field was produced with a Bitter type split coil electromagnet and could be varied continuously up to 12.5 tesla.

4. Discussion of the results.

4.1 EXCHANGE INTERACTIONS AND MAGNON ENERGIES. — Since the concept that $RbMnCl_3$ could be an antiferromagnet with very different near neighbours exchange interactions has not been proven definitively, we will start our analysis of the magnons by adopting a conventional spin wave treatment. Following the authors mentioned in the beginning, this treatment is indeed acceptable for J_1/J_2 values up in the range of 20 [1], a domain which should adequately describe the present situation [2, 3].

We first calculate the various magnon energies for arbitrary values of J_2 and J_1/J_2 by solving the 6 × 6 energy matrix given by Chinn [12] in the case of the the isostructural six magnetic sublattices compound $CsMnF_3$. Figure 7 shows a plot of the reduced zone boundary energies E_2/J_2 for J_1/J_2 going from 1 up to 20. The subscripts a and o stand for the acoustic and optical modes. M, K and A label the points of the Brillouin zone boundary $(2\pi/a\sqrt{3}, 0, 0)$, $(0, 4\pi/3a, 0)$ and $(0, 0, \pi/c)$ where the magnon density of states is highest. The up and down arrows indicate the energetic components resulting from the splitting of the optical branch in the A direction and E_{gap} means the optical energy gap at $k = 0$. These calculations assume negligible anisotropy fields and ferromagnetic interactions.

At this stage, we search for the best fit of our experimental data. Since the location of the hot bands does not depend upon any exciton-magnon interaction, we impose the condition that the lowest and the highest observed frequencies are associated first with $E_{aA} = 32\ cm^{-1}$ and $E_{oA} = 75\ cm^{-1}$. At least for $J_1/J_2 \gtrsim 4$

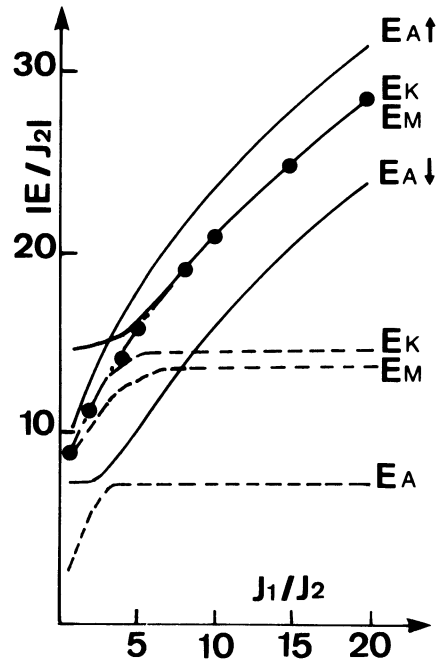

Fig. 7. — Reduced zone boundary magnon energies $E/|J_2|$ *versus* J_1/J_2. The straight and doted lines stand for optical (o) and acoustical (a) modes respectively. The energy gap at $k = 0$ (●●●) follows the relationship $E_g = 3S|J_2|(1 + 2J_1/3J_2)^{1/2}$.

(Fig. 7), E_{aA} does not depend upon J_1/J_2 and we therefore readily get $|J_2| \simeq 4.25\ cm^{-1}$. From E_{oA} we then find $J_1/J_2 \simeq 4.7$ and the corresponding value $J_1 \simeq 20\ cm^{-1}$. The other magnon energies are finally obtained from figure 7 as (Set A) :

$$E_{oK-oM} \simeq 68.9\ cm^{-1}\ ; \quad E_{aK} \simeq 61.1\ cm^{-1}\ ;$$
$$E_{aM} \simeq 55.4\ cm^{-1}\ ; \quad E_{aA} \simeq 42.6\ cm^{-1}\ ;$$
$$\text{and} \quad E_{gap} \simeq 65.6\ cm^{-1}.$$

Alternatively one can keep $E_{aA} \simeq 32\ cm^{-1}$ ($J_2 \simeq -4.25\ cm^{-1}$) and look for a new set of values (Set B) by stating now $E_{oK-oM} = 70\ cm^{-1}$; then we get :

$$J_1/J_2 \simeq 6.2 \quad ; \quad J_1 \simeq 26.35\ cm^{-1}\ ;$$
$$E_{oA} \simeq 76.8\ cm^{-1}\ ; \quad E_{aK} = 61.8\ cm^{-1}\ ;$$
$$E_{aM} \simeq 56.2\ cm^{-1}\ ; \quad E_{oA} \simeq 44.4\ cm^{-1}\ ;$$
$$\text{and} \quad E_{gap} \simeq 67.2\ cm^{-1}.$$

No other set of values for $J_1/J_2 < 4$ could satisfy better the sequence of magnon frequency intervals that we observed in our experiments. Each set A or B reveals the optical origin of the magnon at $\sim 45\ cm^{-1}$, in contradiction with the tentative assignment made by Belyaeva *et al.* [8].

The sidebands located at $\sim 55\ cm^{-1}$ can be associated now, for the first time, with regular acoustic magnon modes.

Altogether the best fit of the optical and magnetic data is obtained for set B. The J_1 and the J_2 values can be further checked by estimating T_N by means of the plot (Fig. 4 of Ref. [2]) giving T_N/J_1 [4] as a function of J_1/J_2. One obtains $T_N \simeq 75.3$-94.2 K with Set B and $T_N \simeq 75.5$-88.9 K with Set A, while the experimental value is ~ 94 K. We wish to stress the fact that the values $J_1/J_2 \simeq 10$ and $J_1 \simeq 29.4\ cm^{-1}$ [4] used previously to analyse magnetization data [3] would lead to the results : $E_{0A} \simeq 69.6\ cm^{-1}$ and $E_{aA} \simeq 22\ cm^{-1}$, for the highest and the lowest magnon frequencies respectively both being substantially lower than the values found from our optical data. These yield, using again the plot of reference 2 [4], $T_N \simeq 57.4$-65.3 K.

Our overall assignments are shown on the right hand side of table I.

4.2 FLUORESCENCE PROCESS. — Turning now our attention to the fluorescence properties, all of the data agree with a complete localization of the optical excitations. Indeed, as in the case of the one and two dimensional antiferromagnets CMC [13], TMMC [14] and $BaMnF_4$ [15], when light is absorbed and emitted by the same manganese ion, the fluorescence lifetime remains the same anywhere across the emission spectrum. This fluorescence lifetime agrees also with the radiative lifetime which can be calculated from the absorption data [16], i.e., $\tau \simeq 1$ ms.

These results differ considerably from those obtained in MnF_2 [16] or $CsMnF_3$ [17] where there is very efficient energy transfers among those manganese ions, linked by strong enough ferromagnetic exchange interactions and to other fluorescing and quenching traps. Exchange energy transfers among antiferromagnetically coupled manganese ions are neglected because of the spin selection rules [13].

In $RbMnCl_3$, as in CMC, TMMC or $BaMnF_4$, only the application of a strong enough magnetic field introduces a high enough ferromagnetic coupling,

by tilting the respective magnetic moments, between those near neighbour manganese ions which were linked by antiferromagnetic exchange at zero field. This allows energy transfers among these ions and/or to other traps. In the absence of other fluorescing centers, this manifests itself in a decrease of the overall intrinsic manganese emission intensity as we observe in our experiments. Subsequently, negligible energy transfers in the absence of an external magnetic field also agree with the assumption made in our spin wave treatment of negligible ferromagnetic interactions.

Acknowledgments.

Thanks are due to R. Mahiou (ERA 1003 CNRS, Lyon) for his assistance with the fluorescence experiments and to U. Kambli-Kallen (Institut fur anorganische une physicalische Chemie, Bern) for sending us a copy of her thesis.

References

[1] SAMUELSEN, E. J. and MELAMUD, M., a) *J. Phys. C.* **6** (1973) 3305 ; b) *ibid.* **7** (1974) 4314.

[2] TAKATORI, S., SUZUKI, N. and MOTIZUKI, K., *J. Phys. Soc. Japan* **50** (1981) 3583.

[3] MOTOKAWA, M., SUZUKI, N. and MOTIZUKI, K., *J. Phys. Soc. Japan* **50** (1981) 3588.

[4] The exchange integrals may be defined in several different ways. In this paper we choose $H = -\Sigma J_{ij} S_i S_j$. Thus our values of J_1 and J_2 are equal to twice those in reference [1-3].

[5] BELYAEVA, A. I., KOTLYARSKII, M. M., STEL'MAKHOV, Yu. N. and MILOSLAVSKAYA, O. V., *Sov. Phys. Solid State* **23** (1981) 726.

[6] BAZHAN, A. N., FEDOSEEVA, N. V., PETROV, S. V. and BEZNOSIKOV, B. V., *Sov. Phys. JETP* **47** (1978) 886.

[7] DIETZ, R. E., MEIXNER, A. E. and GUGGENHEIM, H. J., *J. Lumin.* **1, 2** (1970) 279.

[8] POPKOV, Y. A., BEZNOSIKOV, B. V. and MIL'NER, A. A., *Sov. J. Low Temp. Phys.* **1** (1975) 536.

[9] BELYAEVA, A. I. and KOTLYARSKII, M. M., *Phys. Status Solidi* **B 76** (1976) 419.

[10] BELYAEVA, A. I., KOLTYARSKII, M. M., POPOV, E. A. and EDEL'MAN, S., *Sov. Phys. Solid State* **22** (1980) 379.

[11] KAMBLI-KALLEN, U., Ph. D. Thesis (1983) Bern.

[12] CHINN, S. R., *Phys. Rev.* **B 3** (1971) 121.

[13] BRON, M. Y., EREMENKO, V. V. and MATYUSHKU, E. V., *Sov. J. Low Temp. Phys.* **5** (1979) 502.

[14] YAMAMOTO, H., MC CLURE, D. S., MARZZACO, C. and WALDMAN, M., *Chem. Phys.* **22** (1977) 79.

[15] MONCORGE, R., JACQUIER, B. and MAHIOU, R., DPC Meeting, July 1983. Stanford, California.

[16] WILSON, B. A., HEGARTY, J. and YEN, W. M., *Phys. Rev.* **B 24** (1981) 6725.

[17] MONCORGE, R., JACQUIER, B., MADEJ, C., BLANCHARD, M. and BRUNEL, L. C., *J. Phys.* **43** (1982) 1267.